J. Phys. Chem. Solids Vol. 52, No. 7, pp. 853–857, 1991
Printed in Great Britain.

0022-3697/91 \$3.00 + 0.00
Pergamon Press plc

LINESHAPES OF ESR SIGNALS AND THE NATURE OF PARAMAGNETIC SPECIES IN AMORPHOUS MOLYBDENUM SULFIDES

B. DEROIDE, Y. BENSIMON, P. BELOUGNE and J. V. ZANCHETTA
Université Montpellier 2, Sciences et Techniques du Languedoc, Laboratoire de Physico-chimie des Matériaux, Equipe de Chimie-Physique (URA D0407 CNRS), Place Eugène Bataillon, 34095 Montpellier, Cedex 5, France

(*Received* 11 *October* 1990; *accepted* 23 *January* 1991)

Abstract—Amorphous and poorly crystallized molybdenum sulfides were studied by ESR. Qualitative analysis of the spectra suggests the presence of three paramagnetic species. A simulation of the ESR spectra was attempted on this basis. ESR lines were calculated over the stoichiometry range $MoS_3 \rightarrow MoS_2$. A good representation of the main part of the experimental lines was obtained. There is no significant variation of the g values of the various components of the spectra during the transformation from MoS_3 to MoS_2. The first signal is attributed to sulfur centers. The two others are assigned to metal centers. One is due to Mo^V sites in a chain-like structure, observed in the amorphous phase of MoS_3. The other is due to Mo^V defects in a layered MoS_2 microstructure. The variation of the site concentration was calculated for all compounds, from MoS_3 to MoS_2.

Keywords: Molybdenum sulfides, ESR spectra, paramagnetism, amorphous, chalcogenides.

1. INTRODUCTION

Most hydrocracking catalysts are active because they contain molybdenum sulfides. Industrially they are prepared from oxides which are sulfurised. This leads to non-stoichiometric sulfides, whose study can prove interesting. Catalytic processes depend strongly on the electronic configuration of each component and on the nature of the active species. Thus, we have studied the electronic properties of molybdenum sulfides and, in particular performed ESR experiments in order to confirm the nature of the paramagnetic species responsible for the observed signals.

In previous studies, transport properties of chalcogenides MoS_{2+x} and WS_{2+x} (where $0 \leqslant x \leqslant 1$) were analyzed and the results of ESR powder spectra presented [1–3]. This previous work, based on the analysis of complex spectra, led us to assign to the different components paramagnetic species such as: amorphous S, and oxidized or sulfurized derivatives of Mo^V. The spin concentrations were obtained by numerical integration and compared with the number of sites involved in transport properties. In these ESR investigations, the first analysis of the spectra was too complex to give precise information about the characteristics of these paramagnetic centers.

Trichalcogenides are amorphous. Dichalcogenides remain amorphous after thermal decomposition at low temperature (< 500°C). However, crystallized disulfides are obtained when the temperature is higher than 500°C and when decomposition takes place under sulfur-containing atmosphere. Thus, the degree of crystallinity depends on the experimental procedure. From the study of ESR lines observed for amorphous MoS_3 and MoS_2 and for poorly crystalline MoS_2, the hypothesis of three different paramagnetic species has been proposed [1–3]. In this work, a simulation of the ESR lines is discussed and the evolution of each paramagnetic species with the treatment temperature (*TT*) is presented. The nature of the paramagnetic species will therefore not be discussed. The present work concerns the determination of the contribution of each species to the resonance spectrum, and the simulation of the experimental spectra, in order to confirm the proposed hypothesis.

It is well known that quantitative evaluations of ESR experiments on powders are complex and need numerical treatment. We have selected a simple simulation method which appeared to be rapid and sufficiently precise for this kind of study.

2. SAMPLE PREPARATION AND CHARACTERIZATION

The preparation of chalcogenides MoS_{2+x} with $0 < x < 1$, has been widely described previously [4–8]. The MoS_3 sample was prepared by thermal decomposition of ammonium tetrathiomolybdate at 200°C under dry N_2 for 6 h. This amorphous trichalcogenide has been the subject of several structural investigations, and a chain-like model with paired metal atoms has been established [9–12]. Samples corresponding to the composition MoS_{2+x} were prepared by thermal treatment of MoS_3 between 230°C and 500°C. In this thermal domain, when operating under flowing N_2

Table 1. Stoichiometry of the compounds studied as a function of the treatment temperature TT

Sample	MoS_3	$MoS_{2.75}$	$MoS_{2.65}$	$MoS_{2.6}$	$MoS_{2.2}$	MoS_2	MoS_2
TT(°C)	195	235	285	315	350	440	545

atmosphere, X-ray spectra are always characteristic of amorphous compounds. Poorly crystalline solids are obtained in the $500 < TT < 900°C$ domain and well crystallized compounds for $TT > 1000°C$. In these cases, a sulfur-containing atmosphere is required to avoid the formation of metallic molybdenum. From X-ray diffraction analysis of these polycrystalline samples, a hexagonal structure ($2H$) was found. The possible rhombohedral form ($3R$) has not been observed and the diffraction patterns were always broadened, indicating that the solids possess far from perfect crystallinity. Sample significants are reported in Table 1; the stoichiometry was obtained from chemical analysis. Details of the preparative techniques are reported elsewhere [1, 2].

3. EXPERIMENTAL DETAILS

The ESR experiments were performed using an X-band microwave spectrometer, operating at a frequency of $v = 9.6$ Ghz. A double cavity was used for a more accurate determination of the spectroscopic splitting factors. These g values were determined by comparison with DPPH. A numerical double integration was used for the determination of the spin concentration. A more detailed analysis of the method has been described elsewhere [2, 8]. Powdered samples were introduced into silica tubes (internal diameter $\phi = 2$ mm) and sealed under vacuum, the spectra being slightly modified by exposure of the compounds to the air. The operating temperature T was 293 K for all the samples. A microcomputer was used for spectra acquisition. From these data a double numerical integration provided the area of the absorption signal. The number of spins was then determined by comparison with the signal of a secondary standard, Lapis Lazulli, chosen for its width being comparable to those of the samples studied. Its signal is quite intense, symmetric under standard conditions and not air sensitive.

4. SIMULATION OF THE POWDER SPECTRA

The assignments which have been proposed in previous works will be indicated later on. Let us mention here, however, that the nature of the spectra suggested the presence of three paramagnetic species in the compounds MoS_{2+x} (Fig. 1). It is clear that the contribution of different components makes the spectra difficult to analyze quantitatively. Indeed, the components of the anisotropic g tensor of each species cannot be directly obtained and a simulation is needed to verify the validity of the hypothesis of three paramagnetic species. No hyperfine structure was observed and the magnetic properties of the Kramer doublets were simply described with a completely anisotropic g tensor ($g_x \neq g_y \neq g_z$).

The calculation of the theoretical ESR spectra has been carried out elsewhere [12–15]. For the ith species the lineshape of the integral curve is obtained by integrating the transition probability $P(\vartheta, \varphi)$ over all the ϑ, φ space:

$$I_i(H) = \int_0^{\pi}\int_0^{2\pi} P(\vartheta, \varphi) L(H - H^*) \sin\vartheta \, d\vartheta \, d\varphi, \quad (1)$$

where $L(H - H^*)$ is the lineshape function and H^* the effective value of the field for the g value.

It has been shown [14, 15] that $P(\vartheta, \varphi)$ can be written:

$$g^2 \times P(\vartheta, \varphi) = g_x^2 g_y^2 (1 - l_z^2) + g_y^2 g_z^2 (1 - l_x^2) + g_x^2 g_z^2 (1 - l_y^2), \quad (2)$$

where l_x, l_y and l_z are the direction cosines between the applied field H and x, y and z; therefore the g modulus is classically calculated as:

$$g^2 = g_x^2 l_x^2 + g_y^2 l_y^2 + g_z^2 l_z^2. \quad (3)$$

The calculation of $I_i(H)$ is not simple and needs numerical integration over all ϑ and φ directions. The following method has been developed by several authors [13, 14]. When the lineshape degenerates to a Dirac peak, expression (1) becomes:

$$\Delta_i(H) = \int_0^{\pi}\int_0^{2\pi} P(\vartheta, \varphi) \frac{\delta(H - H^*)}{\beta g} \sin\vartheta \, d\vartheta \, d\varphi, \quad (4)$$

where β is the Bohr magneton and the βg factor is introduced for normalization [16, 17]. This equation can be expressed by elliptic integrals (see, for example, Ref. 18), and numerical tables or polynomial approximations provide a very good approximation of these integrals. From this stick diagram we return to the absorption spectrum of the ith species by a product of convolution with the lineshape function L:

$$I_i(H) = \int_0^{\infty} \beta g \, \Delta_i(H_m) L(H - H_m) \, dH_m. \quad (5)$$

We verified that a Gaussian lineshape function was not adequate for this simulation; a more accurate fitting was obtained with the Lorentzian function:

$$L(H - H_m) = \frac{1}{\pi\sigma} \frac{1}{1 + \dfrac{(H - H_m)^2}{\sigma^2}}, \quad (6)$$

where σ is the width for the individual lines.

The same calculation was carried out for each paramagnetic species, and the spectrum $I(H)$, resulting in the contribution of each paramagnetic species, is given by:

$$I(H) = \sum_{i=1}^{3} \alpha_i I_i(H), \quad (7)$$

where α_i is the relative strength coefficient of each species to the absorption, such that:

$$\sum_{i=1}^{3} \alpha_i = 1. \quad (8)$$

5. RESULTS AND DISCUSSION

Basic hypothesis

The simultaneous presence of paramagnetic S and Mo (or W) was suggested in previous work on MoS_{2+x} (or WS_{2+x}) [2, 7]. A comparison with ESR results observed on molybdenum oxides [19, 22] confirms the presence of paramagnetic molybdenum in both oxides and sulfides. But the spectra differ for g values greater than 2. The spectra of sulfides are always more complex and qualitative analysis led us to consider the presence of three different paramagnetic species: one due to sulfur (signal S) and two due to molybdenum (A and B) [7, 8].

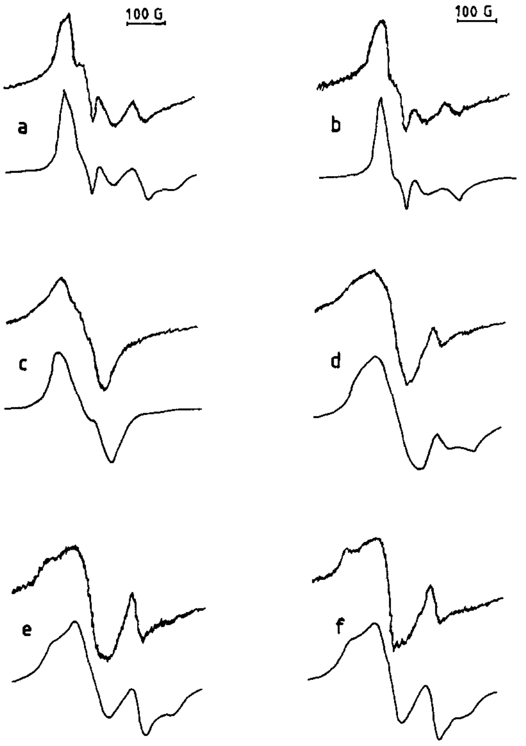

Fig. 1. ESR spectra of amorphous molybdenum sulfides prepared at: (a) $TT = 200°C$; (b) $TT = 235°C$; (c) $TT = 285°C$; (d) $TT = 350°C$; (e) $TT = 440°C$ and (f) $TT = 545°C$. For each TT, the upper curve is the experimental one and the lower, the calculated line. Experimental conditions: temperature $T = 295$ K; central magnetic field: 3450 G; microwave frequency: 9.56 GHz.

Results

ESR spectra were taken at room temperature. The precursor of the compounds is the thiosalt $(NH_4)_2MoS_4$. The weak ESR signal observed for this compound is assigned to a surface decomposition and the density of spins is too weak to be evaluated with accuracy. Figure 1 presents some typical spectra obtained with amorphous molybdenum sulfides. The similitude of the spectra can be seen throughout the composition range $MoS_3 \rightarrow MoS_2$. We also notice the evolution of the line intensities when TT increases between 195°C and 545°C: they decrease when TT increases for $g > 2$, while they remain well resolved up to 545°C for $g < 2$. In contrast, the compounds prepared by thermal treatment in sealed silica tubes at $TT \geqslant 700°C$ do not show any ESR signal. The total number of sites has been calculated for solids prepared between 195°C and 545°C, according to the method described previously. The results are presented in Fig. 2. They are in good agreement with our previous measurement [2]. The densities of the sites are always greater in these compounds than in tungsten sulfides, which have similar structures.

In accordance with the basic hypothesis, a simulation of the ESR spectra was carried out with three distinct paramagnetic species. Whatever the treatment temperature TT, a good fit of experimental curves was obtained. This is illustrated in Fig. 1, where calculated curves are compared to the experimental spectra. Compared to the calculated curves, a broadening effect on the edges of the spectra is observed. However, a good agreement is obtained in the central part of the curves, intensities as well as g values of the extrema being comparable.

The fitting values gx, gy, gz and the individual lineshape factors σ are listed in Table 2. It should be

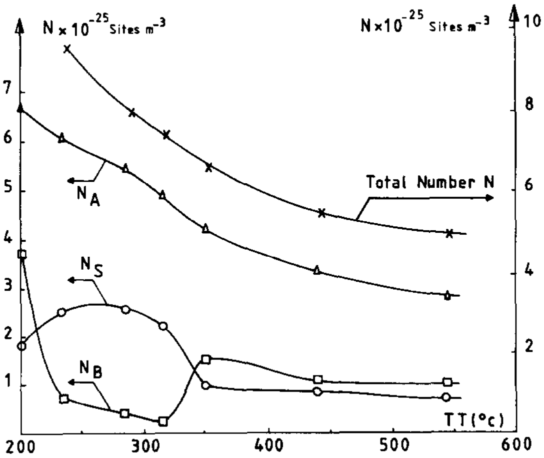

Fig. 2. Total number of paramagnetic centers and number of each species as a function of the temperature TT. N_A and N_B are relative to molybdenum sites named A and B. N_S is relative to sulfur centers.

Table 2. Summary of the values of the ESR parameters used to simulate the spectra of amorphous samples MoS_3 to MoS_2. σ is the width of individual lines, N_s, N_A and N_B are the numbers of sites of each species

Sample	MoS_3	$MoS_{2.75}$	$MoS_{2.6}$	$MoS_{2.25}$	MoS_2 (440°C)	MoS_2 (545°C)	
	g_x	2.003	2.003	2.003	2.003	2.003	2.003
	g_y	2.029	2.029	2.029	2.030	2.035	2.035
Signal S	g_z	2.045	2.045	2.050	2.055	2.062	2.062
	σ(gauss)	10	10	20	25	30	30
	$N_S 10^{-22}(mol^{-1})$	0.16	0.21	0.15	0.06	0.05	0.04
	$N_S 10^{-25}(m^{-3})$	1.8	2.5	2.2	0.95	0.85	0.75
	g_x	1.927	1.927	1.970	1.950	1.927	1.927
	g_y	1.987	1.987	1.987	1.990	1.992	1.992
Signal A	g_z	2.024	2.024	2.024	2.024	2.024	2.024
	σ(gauss)	25	25	35	35	30	30
	$N_A 10^{-22}(mol^{-1})$	0.6	0.52	0.34	0.26	0.22	0.2
	$N_A 10^{-25}(m^{-3})$	6.7	6.1	4.9	4.2	3.3	3.0
	g_x	1.885	1.885	1.885	1.885	1.885	1.885
	g_y	1.940	1.940	1.940	1.940	1.940	1.940
Signal B	g_z	1.942	1.942	1.942	1.942	1.942	1.942
	σ(gauss)	35	35	30	30	30	30
	$N_B 10^{-22}(mol^{-1})$	0.34	0.05	0.01	0.1	0.08	0.07
	$N_B 10^{-25}(m^{-3})$	3.8	0.6	0.15	1.5	1.2	1.11

noted that g values are almost constant for signals A and S, and constant in the case of B, when *TT* increases. This fact justifies the choice of a model with three distinct paramagnetic species. Typical values of α are 0.14, 0.55 and 0.31, respectively, for signals S, A and B.

Within the framework of this model, the number of each paramagnetic species A, B and S can be obtained from the values α used in eqn (7). These are shown in Fig. 2 as a function of *TT*.

Paramagnetic sulfur in MoS_{2+x}

With a view to characterizing the sulfur sites, measurements were first made on vitreous sulfur. Sulfur is amorphous when it is prepared by quenching the melt first heated above 200°C. No ESR signal is then observed under standard conditions. Paramagnetism is observed when the sample is irradiated with u.v. light at $T = 77$ K. Dependence of the amplitude on the time of the u.v. exposure is observed. The line shape is typical of a totally anisotropic medium. Although previous work suggested the presence of distinct sites [23], a single asymmetric g tensor was used to take this signal into account.

The best adapted values of g are listed in Table 3 and compared with an earlier study. This table also provides sulfur g values (signal S) used in the case of MoS_3. The trisulfide was also irradiated under the same conditions with no variation in the intensities of the spectra observed. This method is probably not sensitive enough to reveal the eventual presence of free sulfur chains. The ESR signal ascribed to sulfur remains after high treatment temperatures. This observation seems to exclude the presence of radicals related to S_8 rings. Therefore it is likely that this ESR absorption is due to short chains. The presence of a paramagnetic signal at room temperature certainly results from short chains stabilized by the local structure of the solid.

Paramagnetic Mo *in* MoS_{2+x}

The first paramagnetic Mo^V (signal A) is observed from the lowest to the highest values of *TT*, with a regular decrease of the intensity when *TT* increases. There is a loss of resolution of the line when the stoichiometry of S/Mo = 2 is reached.

The second paramagnetic Mo^V (signal B) is less intense and can be observed all over the temperature range investigated. Its resolution is improved for $TT \geqslant 300$°C. It disappears when X-ray diffraction analysis indicates a good polycrystalline layered structure.

Table 3. Values of the observed paramagnetic parameters of sulfur centers in amorphous sulfur and in MoS_3. g_m is defined as: $g_m = 1/3(g_x + g_y + g_z)$

Source	Sample	g_x	g_y	g_z	g_m	σ_{gauss}
This work	S vitreous	2.038	2.021	2.001	2.020	7
Ref. 23	S vitreous	2.041	2.026	2.003	2.023	—
This work	S in MoS_3	2.045	2.029	2.003	2.027	10

Taking into account the results of microstructural studies on these chalcogenides, the nature of paramagnetic molybdenum can be specified. As already mentioned [9–11], from the analysis of X-ray radial distribution functions, X-ray photoelectron spectroscopy and EXAFS measurements, a chain-like structure in amorphous WS_3 and MoS_3 has been established. According to this model, the structure is based on two trigonal sulfur prisms opposed by an atom of molybdenum. Spin paired Mo–Mo are formed along the chain so that two different Mo–Mo distances are observed. At the same time, sulfide and disulfides are obtained in the chain.

Any local defect in this structure, i.e. a cut-off in the chain or a dangling bond, provides a paramagnetic molybdenum site. With this microscopic model, this site has a local anisotropy and therefore can be characterized by an anisotropic g tensor. The paramagnetic sites (named A) with $g_x \neq g_y \neq g_z$, mainly observed when the stoichiometry is close to MoS_3, are due to this type of defect.

When prepared at higher temperature *TT*, dichalcogenides MoS_2 can be obtained with a layered structure [2, 4]. In this $2H$ structure, the elementary cell consists of trigonal prisms containing one molybdenum and six sulfurs. No ESR signal is observed on well organized disulfides, but paramagnetic Mo can be observed in poorly crystalline disulfides, as well as in MoS_{2+x}. Amorphous MoS_2 consists of crystalline microdomains with a layered structure, presenting different sizes and stacking defects [24]. A paramagnetic metallic size Mo^V is then characterized by an environmental symmetry of axial type with $g_y = g_z$. The Mo^V signals (named B, not observed in oxides) are attributed to these sites. They are not observed when $TT \geqslant 700°C$: the growth of the crystallite sizes and the decrease of stacking defects explain the decrease of the B defects in this thermal domain. Their number is correlated to the crystallinity of the samples.

When samples are oxidized at low temperature, the ESR spectra are modified and the assignments of signals are confirmed. In the same way, sensitivity to hydration is observed by ESR on these oxides [8]. It acts selectively and the results are in agreement with the assumption of three paramagnetic sites. This work is underway and will be presented later.

6. CONCLUSION

Amorphous molybdenum sulfides and poorly crystallized molybdenum disulfides present ESR sites which are Mo or S species. Two types of paramagnetic Mo^V are observed and their experimental variation with *TT* has been described.

There is no support for the presence of free sulfur chains in these sulfides. The paramagnetic sulfur seems to be in MoS_3 chains, and the amplitude of the S signal decreases when the A signal decreases.

Throughout the stoichiometry $3 < S/Mo < 2$, we observed the presence of signals A and B simultaneously.

As a first conclusion, these two results act in favour of a biphasic model of the materials. Even in the case of MoS_3, the B signal, due to layered MoS_2 microcristallites is observed, although the MoS_2 phase with a chain-like structure is predominant. From this result, MoS_{2+x} seems to be a biphasic compound $MoS_3 + MoS_2$. In layered compounds MoS_2, only the poorly crystalline samples present paramagnetic sites B. The catalytic properties of these amorphous disulfides may be related to these paramagnetic sites.

A simple model of three anisotropic g tensors was used for modeling the ESR spectra. Although this model is a simple one, it was possible to take into account the spectra of all the samples studied. It must be possible to apply this method to other spectra of amorphous compounds and obtain further results on the nature of paramagnetic species. This analysis of ESR spectra may also give further indication about the microstructure of amorphous compounds.

REFERENCES

1. Bensimon Y., Belougne P., Giuntini J. C. and Zanchetta J. V., *J. phys. Chem.* **88,** 2754 (1984).
2. Deroide B., Belougne P. and Zanchetta J. V., *J. Phys. Chem. Solids* **48,** 1197 (1987).
3. Busetto L., Vaccari A. and Martini G., *J. phys. Chem.* **88,** 1927 (1984).
4. Muller A., Diemann E. and Baran E. Z., *Z. Anorg. Allg. Chem.* **87,** 375 (1970).
5. Prasad T. P., Diemann E. and Muller A. J., *Inorg. Nucl. Chem.* **35,** 1895 (1973).
6. MacDonald J. W., Friesen G. D., Rosenheim L. D. and Newton W. E., *Inorg. Chim. Acta.* **72,** 205 (1983).
7. Deroide B., Thèse d'Etat Montpellier (1986).
8. Bensimon Y., Thèse d'Etat Montpellier (1989).
9. Voorhoeve R. J. H. and Wolters H. B. M., *Z. Anorg. Allg. Chem.* **376,** 165 (1970).
10. Liang K. S., deNeufville J. P., Jacobson A. J., Chianelli R. R. and Betts F., *J. Non-Cryst. Sol.* **35, 36,** 1249 (1980).
11. Liang K. S., Cramer S. P., Johnston D. C., Chang C. H., Jacobson A. J., deNeufville J. P. and Chianelli R. R., *J. Non-Cryst. Sol.* **42,** 345 (1980).
12. Pilbrow J. R., *Molec. Phys.* **16**-3, 307 (1969).
13. Kodratoff Y., Meriaudeau P. and Imelik B., *J. Chim. Phys.* **68,** 1084 (1971).
14. Zimmermann R., *J. Magn. Reson.* **49,** 425 (1982).
15. Kneubühl F. K., *J. chem. Phys.* **33,** 1074 (1960).
16. Aasa R. and Vänngård T., *J. Mag. Res.* **19,** 308 (1975).
17. Isomoto A., Watari H. and Kotani M., *J. Phys. Soc. Japan* **29,** 1571 (1970).
18. Abramovitch M. and Stegun L. A., *Handbook of Mathematical Functions*, 8th edition (1968).
19. Dufaux M., Che M. and Naccache C. J., *J. Chim. Phys.* **67,** 527 (1980).
20. Ueda H. and N. Todo N., *J. Catal.* **27,** 281 (1972).
21. Vedrine J. C. and Praliaud D. H., *Surf. Sci.* **80,** 101 (1979).
22. Hagenbach G., Menguy P. and Delmon P., *Bull. Soc. Chim. Belg.* **83,** 1 (1974).
23. Elliott S. R., *J. Phys. Sup.* **10,** 42 C4 384 (1981).
24. Liang K. S., Chianelli R. R., Chien F. Z. and Moss S. C., *J. Non-Cryst. Sol.* **79,** 251 (1986).